Enhancing the Thermoelectric Power Factor with Highly Mismatched Isoelectronic Doping

Joo-Hyoung Lee,[1,4] Junqiao Wu,[1,2,3] and Jeffrey C. Grossman[4]

[1]*Berkeley Nanosciences and Nanoengineering Institute, University of California, Berkeley, California 94720, USA*
[2]*Department of Materials Science and Engineering, University of California, Berkeley, California 94720, USA*
[3]*Materials Science Division, Lawrence Berkeley National Laboratory, Berkeley, California 94720, USA*
[4]*Department of Materials Science and Engineering, Massachusetts Institute of Technology, Cambridge, Massachusetts 02139, USA*

(Received 16 July 2009; published 8 January 2010)

We investigate the effect of O impurities on the thermoelectric properties of ZnSe from a combination of first-principles and analytic calculations. It is demonstrated that dilute amounts of O impurities introduce peaks in the density of states (DOS) above the conduction band minimum, and that the charge density near the DOS peaks is substantially attracted toward O atoms due to their high electronegativity. The impurity-induced peaks in the DOS result in a sharp increase of the room-temperature Seebeck coefficient and power factor from those of O-free ZnSe by a factor of 30 and 180, respectively. Furthermore, this effect is found to be absent when the impurity electronegativity well matches the host that it substitutes. The results suggest that highly electronegativity-mismatched alloys can be designed for high performance thermoelectric applications.

DOI: 10.1103/PhysRevLett.104.016602 PACS numbers: 72.20.Pa, 71.15.−m, 71.55.Ht

For many years, defects in semiconductors have been intensively studied both theoretically and experimentally in various dimensionalities such as zero- (point defects), one- (line defects), and two-dimensional (stacking fault and grain boundaries) forms due to their ability to modify mechanical, electrical, and optical properties of the host semiconductors [1–8]. Among these, point defects such as impurities are of particular interest because they provide control over the electrical conductivity by several orders of magnitude in the form of doping [4]. Recently, defects were also utilized to improve thermoelectric efficiency, which is described by the thermoelectric figure of merit $ZT = S^2\sigma T/\kappa$. Here, S is the Seebeck coefficient or thermopower, σ the electrical conductivity, T the absolute temperature, and κ the total thermal conductivity given as the sum of the electronic (κ_e) and lattice (κ_l) contributions, respectively. It is noted that while $ZT > 3$ is needed for thermoelectric materials to compete with conventional equipment, ZT has remained around 1.0 for many years due to the difficulty in optimizing S, σ and κ arising from their interdependence [9]. Okinaka *et al.* showed [10] that the Seebeck coefficient of TiO containing additional oxygen atoms exhibits a sharp increase by a factor of 80 compared to that of stoichiometric TiO, resulting in $ZT = 1.64$ at 800 °C, which is among the largest ZT values reported in this temperature range.

In addition to the improvement of thermoelectric properties in metal oxides, Heremans *et al.* demonstrated [11] that ZT of Tl-doped PbTe reaches 1.5 at 773 K which is twice as large as that of the best conventional p-type PbTe-based alloys. This improvement in ZT results from an increase in S, caused by additional Tl-induced peaks in the density of states (DOS). While the precise origin of the additional energy levels is still under investigation, these results are in agreement with theoretical considerations by Mahan and Sofo [12], who predicted that a sharp increase in the DOS would improve thermoelectric efficiency by enhancing the Seebeck coefficient.

In fact, a broad class of materials exists that is known to be capable of achieving wide control over the electronic structures and DOS [13]. Such control stems from the alloying of isovalent but highly electronegativity-mismatched constituents at dilute concentrations, forming a system known as highly mismatched alloys (HMAs). In HMAs, the hybridization between the extended states of the majority component and the localized states of the minority component results in a strong band restructuring, leading to peaks in the DOS and new subbands near the original conduction or valence band edge. These narrow subbands formed in HMAs have a heavy effective carrier mass due to their localized origin, and give rise to a sharp DOS distinct from those of the host material. The resultant modifications in optical and electronic properties have been studied for optoelectronics applications in Group IV, III-V, and II-VI HMAs such as $Ge_{1-x}Sn_x$ [14], $GaN_{1-x}As_x$ [15,16], and $ZnTe_{1-x}Se_x$ [17]. Although the potential for enhancing the thermopower is expected from such a restructured DOS, the nature and magnitude of the enhancement as well as the subsequent effect on the power factor has not been fully understood within an atomic-scale electronic structure framework. It is thus particularly interesting to understand and explore possibilities of impurity-induced peaks in the DOS with a view of improving thermoelectric efficiency, as it could provide another independent route to enhance ZT besides the widely adopted approaches that rely on reducing κ [18–20].

In this work, $ZnSe_{1-x}O_x$ is used as a model HMA to investigate the effect of a highly mismatched isoelectronic impurity (in this case, oxygen) on thermoelectric properties based on first-principles density functional theory

(DFT) [21]. We consider two different concentrations (x) of O impurities ($x = 3.125$ and 6.25%) which substitute Se atoms in a $2 \times 2 \times 2$ supercell. It is demonstrated that O atoms introduce peaks in the DOS above the conduction band minimum (CBM), and that the charge density near the DOS peak is well localized around O atoms because of their high electronegativity. We predict that the room-temperature Seebeck coefficient of $ZnSe_{1-x}O_x$ is substantially enhanced compared to that of ZnSe due to the peaks in the DOS, which consequently results in a sharp increase in the power factor. Taken together, these results suggest that controlling features in the DOS via hybridization between impurity states and extended CBM levels could be an important direction to design new materials for improving thermoelectric efficiencies.

The total DOS of $ZnSe_{1-x}O_x$ (Fig. 1) shows that O impurities introduce peaks in the conduction band. For $x = 3.125\%$, a sharp peak appears at 1.1 eV above the CBM, which corresponds to a carrier concentration (n_e) $\sim 1.1 \times 10^{21}$ cm^{-3}, while the case with $x = 6.25\%$ has peaks at 1.2 and 1.3 eV above the CBM, corresponding to $n_e \sim 1.3 \times 10^{21}$ cm^{-3} and 2.3×10^{21} cm^{-3}, respectively. The projected DOS (PDOS) further reveals that these peaks are caused by the s states of the O atoms which are located essentially at the DOS peaks in energy [21]. It should be noted that while there are other peaks at higher energies, the peaks described here are of primary interest for thermoelectric properties.

The computed charge densities near the DOS peaks in energy show that the high density region is strongly confined around O atoms with a spherical distribution [21]. The charge density at the O-Zn bond indicates a distorted sp^3 character and is attracted toward O atoms due to the higher electronegativity of oxygen, leading to a strong hybridization between the O impurity states and states in the conduction band of ZnSe. As a result, peaks are induced in the partial DOS of the Zn atoms surrounding O atoms *at the same energy* as those of O s states.

The strong hybridization between the localized states of the O impurity and the conduction band states of the host material can be described within the many-impurity Anderson model [22,23], and results in the so-called band-anticrossing (BAC) effect [24,25], which describes a splitting of the conduction band into two subbands. As is seen from the computed band structures (Fig. 2), even a dilute amount of substitutional O impurity in ZnSe causes significant BAC: while the conduction bands are highly degenerate with no impurities ($x = 0$), for instance, the lowest band along $X \rightarrow M$ and the second lowest band along $\Gamma \rightarrow X$ [Fig. 2(a)] are well split for $x = 3.125\%$ by BAC Fig. 2(b)].

In order to understand the effects of O impurities on the room-temperature thermoelectric properties of ZnSe, we compute σ, and S from the solution of the Boltzmann transport equation by defining the "transport distribution function" [12] within a constant relaxation time approximation. It should be noted that while the relaxation time is taken to be energy-independent, it is given as a function of carrier concentration by fitting available experimental data of free carrier mobility [26,27] for ZnSe through the well-known Caughey-Thomas expression [28]. The conductivity and Seebeck coefficient are calculated by integrating the transport distribution over the Fermi-distribution window. Alloy scattering is neglected in the calculation of electrical conductivity.

Figure 3 shows S and the power factor, $S^2\sigma$, of $ZnSe_{1-x}O_x$ as a function of carrier concentration for n-type doping. As is clear from Fig. 3(a), S is very similar among different x values for $n_e \lesssim 3.0 \times 10^{20}$ cm^{-3}, above which $|S|$ is sharply increased with O impurity present compared to pure ZnSe: for $x = 3.125\%$, $|S|$ is 30 times as large as that of ZnSe at $n_e = 1.2 \times 10^{21}$ cm^{-3}. It is interesting to observe that S changes its sign with O impurities as n_e increases, which could imply technological importance because it provides a possibility to achieve

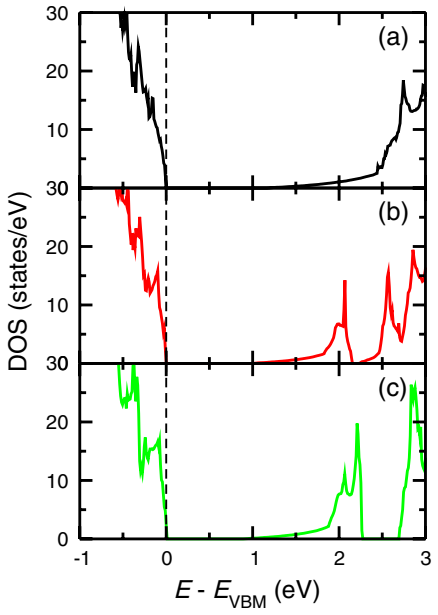

FIG. 1 (color online). Density of states (DOS) per unit cell of $ZnSe_{1-x}O_x$ for (a) $x = 0$, (b) $x = 3.125\%$, and (c) $x = 6.25\%$. The valence band maximum, which is represented by a dotted, vertical line, is aligned for comparison purposes.

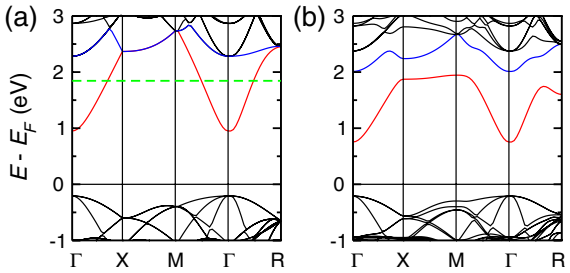

FIG. 2 (color online). Band structures with respect to the Fermi energy (E_F) of $ZnSe_{1-x}O_x$ with (a) $x = 0$ and (b) $x = 3.125\%$. The dotted, horizontal line in (a) represents the computed O impurity level.

both positive and negative thermopower in n-type ZnSe by tuning the doping levels. This peculiar behavior can be understood using the Mott formula [29]:

$$S = \gamma\left(\frac{1}{\sigma(\varepsilon)}\frac{d\sigma(\varepsilon)}{d\varepsilon}\right)_{\varepsilon=\varepsilon_F} = \gamma\left(\frac{1}{D(\varepsilon)}\frac{dD(\varepsilon)}{d\varepsilon} + \frac{1}{f(\varepsilon)}\frac{df(\varepsilon)}{d\varepsilon} + \frac{1}{\mu(\varepsilon)}\frac{d\mu(\varepsilon)}{d\varepsilon}\right)_{\varepsilon=\varepsilon_F}. \quad (3)$$

Here, $\gamma = \pi^2 k_B^2 T/3q$ with q being the carrier charge, k_B the Boltzmann constant, and T the absolute temperature, respectively; $\sigma(\varepsilon) = D(\varepsilon)f(\varepsilon)\mu(\varepsilon)$ where $D(\varepsilon)$, $f(\varepsilon)$, and $\mu(\varepsilon)$ are the density of states, the Fermi distribution and the energy-dependent mobility, respectively, and the derivatives are evaluated at the Fermi energy, ε_F. It is not difficult to see from Eq. (3) that the variation in the DOS is likely to make the largest contribution to the change in S. Because O impurities introduce peaks in the DOS, $dD(\varepsilon)/d\varepsilon$ becomes positive or negative depending on the position of the Fermi energy with respect to the position of the peak. This is more apparent for $x = 3.125\%$, in which case a δ-function-like peak in the DOS (see Fig. 1) leads to a sharp increase in S around $n_e = 1.1 \times 10^{21}$ cm^{-3}.

Figure 3(b) shows the power factor of $ZnSe_{1-x}O_x$, which is significantly enhanced with respect to that of pure ZnSe by a factor of 180 in the peak region for $x = 3.125\%$. We note that this increase in the power factor arises from a relatively high σ for $ZnSe_{1-x}O_x$ as well as large $|S|$ values. As previously discussed, the charge density is strongly localized around the O impurity near the DOS peak, which normally implies significant reduction in σ although $|S|$ is substantially increased. However, it is found that while σ is calculated to be 4.6×10^4 S/cm for ZnSe at the energy corresponding to the DOS peak, it is decreased only by a factor of 5 to 8.5×10^3 S/cm for $x = 3.125\%$, in contrast to the factor of 30 enhancement in $|S|$. This is due to the fact that unlike the DOS peak, which is derived from the localized O s states, carrier transport is governed by hybridization between the impurity wave function near the DOS peak and extended states of the host material, as opposed to hopping conduction between the impurity atoms.

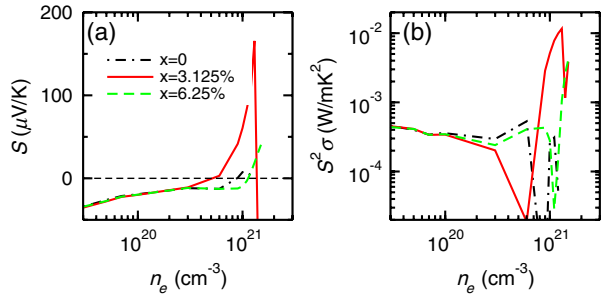

FIG. 3 (color online). (a) Seebeck coefficient, S, and (b) power factor, $S^2\sigma$, of n-type $ZnSe_{1-x}O_x$ as a function of carrier concentration.

It is of interest to see that while the case with $x = 6.25\%$ also possesses peaks in the DOS, the resulting S is not as large as the one for $x = 3.125\%$, due to the fact that the power factor depends on the magnitudes of $D(\varepsilon)$ [30] as well as its shape as proposed by Mahan and Sofo. As is seen from Fig. 1, the DOS peak at $x = 3.125\%$ bears more resemblance to a δ function, which was predicted to produce a maximum increase in the power factor [12], than the ones for $x = 6.25\%$. In addition, the DOS at the peak for $x = 3.125\%$ is about 8.2 times larger than that of ZnSe, whereas the case with $x = 6.25\%$ shows an increase in the DOS by a factor of 5.7 with respect to the $x = 0$ case.

It should be noted that the O impurity level, which is calculated to be about 1.1–1.3 eV above the CBM, is largely overestimated compared to experiments (0.2 eV above the CBM) [25]. This discrepancy originates from the use of a small supercell (64 atoms/cell) employed in the present work as demonstrated by Li and Wei, who showed that a relatively converged value (0.11 eV above the CBM) for the O impurity level in $ZnSe_{1-x}O_x$ is obtained with a 4096-atom supercell [31]. While fully first-principles calculations with the same computational approach as in the present study are extremely challenging for such large systems, $|S|$ is expected to be still largely enhanced with O atoms even when a larger supercell is considered because the DOS peaks will still occur due to a strong hybridization between the O atoms and extended bands of the host, as demonstrated experimentally [25]. Furthermore, if the DOS peaks are located at around 0.2 eV as shown in experiments, the required carrier concentrations for displacing the Fermi level to the DOS peaks would also be significantly reduced.

In order to quantitatively evaluate these corrections, we performed analytical calculations using the Green's function approach in an extended BAC model. Figure 4(a) shows the DOS of $ZnSe_{1-x}O_x$ for $x = 0.03$, calculated from the Green's function approach [22] using the experimental band gap of ZnSe and O impurity level [25,32]. As can be seen, the O impurity induces a strong DOS peak in agreement with the first-principles calculations. Further assuming a constant relaxation time, S is calculated by employing the Mahan-Sofo formulation and presented in Fig. 4(b). As is clear from Fig. 4(b), S shows a similar change in sign and enhancement for $ZnSe_{1-x}O_x$ as in the first-principles calculations: at its maximum, $|S|$ of $ZnSe_{1-x}O_x$ is increased roughly 28 times compared to that of ZnSe. However, the carrier concentration for the largest $|S|$ is 1.7×10^{20} cm^{-3}, an order of magnitude lower than the DFT value, which makes doping for enhancing $|S|$ more realistic and appealing. It should be noted that doping $ZnSe_{1-x}O_x$ can be achieved by introducing halogen atoms: the computed DOS with 0.8% substitution of a halogen atom (F, Cl, Br, or I) at a Se site for $x = 3.125\%$ remains essentially the same as without the dopants around the DOS peaks in energy [21].

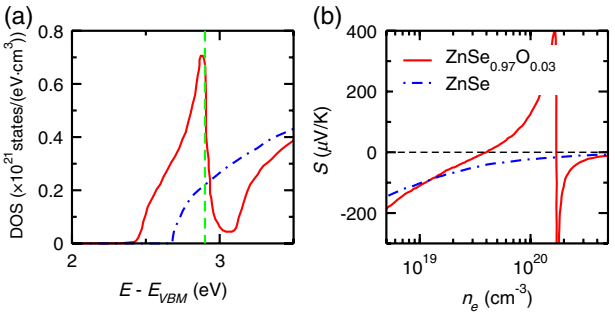

FIG. 4 (color online). (a) DOS of $ZnSe_{0.97}O_{0.03}$ and (b) Seebeck coefficient based on a Green's function calculation with the Mahan-Sofo formulation. The dotted, vertical line in (a) represents the O impurity level.

In order to further explore the role of impurities in this effect, we examined other substitutional impurities such as S with the same concentration as oxygen. Unlike O defects, however, no peak structures in the DOS are observed with S substitution. In fact, the DOS of $ZnSe_{1-x}S_x$ is very similar to that of ZnSe. The dissimilarity in the DOS restructuring between O and S impurities in ZnSe arises from the difference in the electronegativity. While the electronegativity of S is 2.589 [33], close to that of Se (2.434), O has about 48% higher electronegativity than that of Se. The highly mismatched electronegativity of O brings more electrons toward O, leading to strong DOS restructuring as discussed. We also calculated N-F dual impurities in ZnSe instead of two O atoms, and found that the DOS for $ZnSe_{1-x}N_{0.5x}F_{0.5x}$ closely resembles that of $ZnSe_{1-x}O_x$ due to the high electronegativity of N and F, which implies a similar increase in the Seebeck coefficient and power factor.

In summary, we investigated the thermoelectric properties of ZnSe containing anion-substitutional O impurities through first-principles density functional theory and the Boltzmann transport equation. O impurities were shown to introduce DOS peaks within the conduction band, which make $|S|$ and the power factor significantly higher than that of ZnSe at carrier concentrations corresponding to the Fermi level tuned to the peaks. It was also demonstrated that such ability to modify DOS by hybridization with an impurity is absent when the impurity's electronegativity is well matched with the host material. We note that this strategy can be extended to a wide range of HMAs, including those previously mentioned. Unlike PbTe:Tl, these HMAs are all composed of relatively abundant and nontoxic elements. As these HMAs are isoelectronic, introduction of free carriers would require codoping of additional active donors, or, alternatively, HMAs can also be formed with nonisoelectronic doping. These approaches could open a broad avenue toward a variety of abundant materials and new physics for scalable, widely tunable, high-thermopower thermoelectrics.

This work was supported by the National Science Foundation through the Network for Computational Nanotechnology, Grant No. EEC-0634750, and computations were performed at the National Energy Research Scientific Computing Center and Teragrid. J. Wu acknowledges discussions with Dr. W. Walukiewicz, and support from the Laboratory Directed Research and Development Program of Lawrence Berkeley National Laboratory under the Department of Energy Contract No. DE-AC02-05CH11231.

[1] A. J. McGibbon, S. J. Pennycook, and J. E. Angelo, Science **269**, 519 (1995).
[2] C. Molteni *et al.*, Phys. Rev. Lett. **76**, 1284 (1996).
[3] J. M. Carlsson *et al.*, Phys. Rev. Lett. **91**, 165506 (2003).
[4] H. J. Queisser and E. E. Haller, Science **281**, 945 (1998).
[5] F. A. Selim *et al.*, Phys. Rev. Lett. **99**, 085502 (2007).
[6] M.-I. Richard *et al.*, Phys. Rev. Lett. **99**, 225504 (2007).
[7] S. Perraud *et al.*, Phys. Rev. Lett. **100**, 056806 (2008).
[8] Y.-S. Kim and C. H. Park, Phys. Rev. Lett. **102**, 086403 (2009).
[9] A. Majumdar, Science **303**, 777 (2004).
[10] N. Okinaka and T. Akiyama, Jpn. J. Appl. Phys. **45**, 7009 (2006).
[11] J. P. Heremans *et al.*, Science **321**, 554 (2008).
[12] G. D. Mahan and J. O. Sofo, Proc. Natl. Acad. Sci. U.S.A. **93**, 7436 (1996).
[13] J. Wu, W. Shan, and W. Walukiewicz, Semicond. Sci. Technol. **17**, 860 (2002).
[14] K. Alberi *et al.*, Phys. Rev. B **77**, 073202 (2008).
[15] J. Wu *et al.*, Phys. Rev. B **70**, 115214 (2004).
[16] I. Vurgaftman and J. R. Meyer, J. Appl. Phys. **94**, 3675 (2003).
[17] W. Walukiewicz *et al.*, Phys. Rev. Lett. **85**, 1552 (2000).
[18] A. I. Hochbaum *et al.*, Nature (London) **451**, 163 (2008).
[19] A. I. Boukai *et al.*, Nature (London) **451**, 168 (2008).
[20] J.-H. Lee, G. A. Galli, and J. C. Grossman, Nano Lett. **8**, 3750 (2008).
[21] See supplementary material at http://link.aps.org/supplemental/10.1103/PhysRevLett.104.016602 for further details.
[22] J. Wu, W. Walukiewicz, and E. E. Haller, Phys. Rev. B **65**, 233210 (2002).
[23] M. P. Vaughan and B. K. Ridley, Phys. Rev. B **75**, 195205 (2007).
[24] W. Shan *et al.*, Phys. Rev. Lett. **82**, 1221 (1999).
[25] W. Shan *et al.*, Appl. Phys. Lett. **83**, 299 (2003).
[26] N. Shibata, A. Ohki, and A. Katsui, J. Cryst. Growth **93**, 703 (1988).
[27] D. Albert *et al.*, J. Cryst. Growth **159**, 276 (1996).
[28] D. M. Caughey and R. E. Thomas, Proc. IEEE **55**, 2192 (1967).
[29] N. F. Mott and E. A. Davis, *Electronic Processis in Non-crystalline Materials* (Clarendon, Oxford, 1971).
[30] R. Kim, S. Datta, and M. S. Lundstrom, J. Appl. Phys. **105**, 034506 (2009).
[31] J. Li and S.-H. Wei, Phys. Rev. B **73**, 041201(R) (2006).
[32] B. G. Streetman and S. Banerjee, *Solid State Electronic Devices* (Prentice Hall, New Jersey, 2000).
[33] L. C. Allen, J. Am. Chem. Soc. **111**, 9003 (1989).